

Distribution and characteristic of nitrite-dependent anaerobic methane oxidation bacteria in wastewater treatment plants and agriculture fields of northern China

Zhen Hu ^{Corresp., 1}, Ru Ma ¹

¹ School of Environmental Science and Engineering, Shandong University, Jinan, China

Corresponding Author: Zhen Hu
Email address: huzhen885@sdu.edu.cn

Nitrite-dependent anaerobic methane oxidation (n-damo) is a recently discovered biological process, which has been arousing global attention because of its potential in minimizing greenhouse gases emissions. In this study, molecular biological techniques and potential n-damo activity batch experiments were conducted to investigate the presence and diversity of *M. oxyfera* bacteria in paddy field, corn field, and wastewater treatment plant (WWTP) of northern China, as well as lab-scale n-damo enrichment culture. N-damo enrichment culture showed the highest abundance of *M. oxyfera* bacteria and positive correlation was observed between potential n-damo rate and abundance of *M. oxyfera* bacteria. Both paddy field and corn field were believed to be better inoculum than WWTP for the enrichment of *M. oxyfera* bacteria, due to their higher abundance and diversity of *M. oxyfera* bacteria. Comparative analysis revealed that long biomass retention time and optimum environment (low NH_4^+ and high NO_2^- content) were suitable for the growth of *M. oxyfera* bacteria. In addition, the distribution and diversity of *M. oxyfera* bacterial might be related to geographical regions.

1 **Distribution and characteristic of nitrite-dependent anaerobic methane oxidation bacteria by**

2 **comparative analysis of wastewater treatment plants and agriculture fields in northern China**

3 **Zhen Hu^{a,*}, Ru Ma^a**

4 ^a School of Environmental Science and Engineering, Shandong University, Jinan, Shandong, China.

5 Corresponding Author:

6 Zhen Hu

7 *No. 27 Shanda South Road, Jinan, Shandong 250100, China*

8 E-mail: huzhen885@sdu.edu.cn

9

10 Introduction

11 Methane (CH₄) and nitrous oxide (N₂O) are two of the most important greenhouse gases, accounting for about
12 20% and 7% of global warming, respectively (Griggs & Noguer 2002; Knittel & Boetius 2009). Cai (2012)
13 reported that anthropogenic activities, rather than natural sources, are the major sources of CH₄ and N₂O
14 emissions. And it is widely accepted that wastewater treatment plants (WWTPs) and agricultural fields are two
15 of the most important anthropogenic GHGs sources (Foley et al. 2011; Liu et al. 2014a). In WWTPs, enormous
16 amount of CH₄ and N₂O would be produced during the biological transformation of carbohydrates and
17 nitrogenous compounds. Our previous on-site investigation of a typical full-scale WWTP of northern China
18 showed that CH₄ and N₂O emission factors of WWTP were 11.3 g CH₄ person⁻¹ yr⁻¹ and 1.96 g N₂O person⁻¹
19 yr⁻¹, respectively (Wang et al. 2011a; Wang et al. 2011b). Compared with WWTPs, agricultural field is
20 believed to be a more important GHGs sources, mainly because the widely use of fertilizers (IPCC, 2001). It is
21 reported that agriculture field would contribute to 60% of N₂O and 50% of CH₄ emissions on a global scale
22 (Montzka et al. 2011; Syakila & Kroeze 2011).

23 Anaerobic methane oxidation (AMO) is a recently discovered sink of methane on earth, with a
24 consumption rate of approximately 70–300 Tg CH₄ year⁻¹ globally (Cui et al. 2015; Hu et al. 2011). Expect
25 for AMO coupled to sulfate (Barnes & Goldberg 1976; Bian et al. 2001), humic compound (Smemo & Yavitt

26 2007), iron (Beal et al. 2009; Segarra et al. 2013) and manganese (Egger et al. 2015), the coupling of AOM to
27 nitrite reduction process, named nitrite-dependent anaerobic methane oxidation (n-damo), has also been
28 demonstrated (Raghoebarsing et al. 2006). N-damo process was performed by “*Candidatus* Methyloirabilis
29 oxyfera” (*M. oxyfera*), affiliated with the NC10 phylum (Ettwig et al. 2010). N-damo process established a
30 unique relationship between carbon cycle and nitrogen cycle (Raghoebarsing et al. 2006), and it was believed
31 to be a promising method to minimize greenhouse gases emissions through converting CH₄ and N₂O to CO₂
32 and N₂, respectively (Raghoebarsing et al. 2006; Shen et al. 2015).

33 Presently, many studies have been focused on the distribution of *M. oxyfera* bacteria in natural environment,
34 e.g, freshwater lakes (Liu et al. 2014b), paddy soil (Wang et al. 2012), marine sediments (Chen et al.
35 2014), wetlands (Hu et al. 2014b), and etc. However, to date, information about distribution of *M. oxyfera*
36 bacteria in northern China is still lacking. In addition, various inoculums have been reported to be able to
37 successfully enrich *M. oxyfera* bacteria, including freshwater sediment (Raghoebarsing et al. 2006), sewage
38 treatment sludge (Luesken et al. 2011a), ditch sediments (Ettwig et al. 2009) and paddy soil (Shen et al. 2014a;
39 Wang et al. 2012). He et al. (2014) found that inoculum sources had significant effect on enrichment of *M.*
40 *oxyfera* bacteria, and claimed that paddy soil was the optimal inoculum. However, intensive study on inoculum
41 sources from the perspective of microorganism is absence.

42 In this study, the diversity and abundance of *M. oxyfera* bacteria in four different sites of northern China,

43 i.e., paddy field, corn field, n-damo enrichment culture and WWTP, were investigated through molecular
44 biology analyses. Comparative analysis of environmental features and *M. oxyfera* bacteria activity was
45 conducted to reveal the characteristics of *M. oxyfera* bacteria, and optimal enrichment conditions were also
46 proposed.

47 **Materials and methods**

48 *Site description and sample collection*

49 Non-flooded paddy field with rice reaping once per year (PF) and corn field with maize-wheat rotation for over
50 50 years (CF), both of which are typical agricultural type of northern China, were selected as agricultural field
51 sample sites. PF cores and CF cores were collected from three locations (5m distance) at the 50cm-60cm depth
52 in each sampling site, according to the previously described methods (Hu et al. 2014b). Sludge from anaerobic
53 tank of local WWTP (Everbright Water, Jinan China) (WS), and lab-scale Upflow Anaerobic Sludge Bed
54 reactor (UASB) aiming at enrichment of *M.oxyfera* bacteria (EC), were selected as WWTP samples. The
55 sample collection was conducted in October, 2015, and the environmental characteristics of each sample site
56 were listed in Table 1.

57 All collected samples were placed in hermetic containers and immediately transported to the laboratory

58 within 4h. Subsequently, the collected samples were equally divided into three parts. The first part was placed
59 in the incubator to measure the potential n-damo rates, the second parts was stored in refrigerator at 4°C for
60 analysis of physicochemical parameters, and the last part was stored in refrigerator at -20°C for further
61 microbiological analysis.

62 *Table 1. Environmental characteristics of the sample sites*

63 *Physicochemical parameters analysis*

64 Soil samples were extracted with 1M KCl and the concentrations of ammonium, nitrite and nitrate were
65 measured as described by Ryan et al. (2007). Soil pH was measured at soil/water ratio of 1:2.5 using a pH
66 analyzer (HQ30d 53LEDTM, HACH, USA) (Wang et al. 2012). Temperature and salinity of soil was
67 measured *in situ* using HI98331 soil electrical conductivity meter (HANNA, Shanghai).

68 Concentrations of ammonium, nitrite and nitrate in water samples were analyzed according to the standard
69 method (APHA 2005). Water temperature, pH and salinity were measured *in situ* using pH and salinity
70 analyzer (DDBJ-350, Leici, Shanghai). And CH₄ concentration was analyzed using gas chromatograph
71 equipped with flame ionization detector (FID–GC) (7890B, GC system, Agilent Technologies).

72 *Potential n-damo activity batch experiment*

73 All the samples were washed three times with anaerobic water to remove the residual NO_x⁻ (NO₂⁻ and NO₃⁻)

74 and organic compounds, and were then transferred to 1L Ar-flushed glass bottles. The soil slurries were pre-
75 incubated under anoxic conditions for at least 48 h to recover the microbial activity, and then flushed with Ar
76 gas again before the measurement of potential n-damo activity. Two treatment groups were conducted
77 subsequently: (a) CH₄ (blank group, CH₄ at 99%), (b) CH₄+NO₂⁻(experimental group). The initial CH₄
78 concentrations in both blank and experimental groups were 1.02 ± 0.06 mmol L⁻¹ and the initial concentrations
79 of NO₂⁻ in the experimental groups were 0.35 ± 0.01 mmol NO₂⁻ L⁻¹. The variation of CH₄ and NO₂⁻
80 concentrations were determined at intervals of 6 hours. The potential methane oxidation rates and the ratio of
81 CH₄/NO₂⁻ were evaluated by linear regression of the concentrations of decreased CH₄ and NO₂⁻ in the
82 experimental groups.

83 *Fluorescence in situ hybridization (FISH)*

84 Approximately 0.3g of collected samples were washed in phosphate-buffered saline (PBS; 10 mM
85 Na₂HPO₄/NaH₂PO₄ pH 7.5 and 130 mM NaCl) and fixed with 4% (w/v) paraformaldehyde in PBS for 3h under
86 4°C. After incubation, the sediment (fixed biomass) was washed with PBS and then stored in mixture (1ml) of
87 ethanol and PBS (1×) at -20 °C until analysis.

88 Bacterial probe S⁻-DBACT-1027-a-A-18 (5'-TCTCCACGCTCCCTTGCG-3') (Cy3, red), specific for
89 bacteria affiliated with the NC10 phylum were used in this study (Raghoebarsing et al. 2006); and a mixture of

90 EUB I-III (FITC, green) was used for the detection of total bacteria (Daims et al. 1999). Fixed biomass (10 µl)
91 was spotted on microscopic slides circles and then dehydrated subsequently with 50%, 80%, and 98% of
92 ethanol for 3min each. The probes were hybridized for 2 h at 46 °C in hybridization buffer (5M NaCl, 1M
93 Tris/HCl pH 8.0, 10% sodium dodecyl sulfate) and 40% formamide. Hybridized samples were washed with
94 hybridization leachate at 48°C and then added with the fluorescence decay resistance agent. Fluorescence
95 microscope (Olympus BX53, Japan) was used to observe the prepared slides and the picture was disposed with
96 software Image-Pro Plus 6.0.

97 *DNA extraction and PCR amplification*

98 Total DNA was extracted using Power Soil DNA Isolation kit (Mo Bio Laboratories, Carlsbad, CA) according
99 to the manufacturer's protocols. And DNA concentration was measured at 260nm with Nano-drop
100 spectrophotometer (Nano-Drop Technologies, USA).

101 To understand the biodiversity of *M. oxyfera* bacteria, 16S rRNA gene and *pmoA* gene of *M. oxyfera*
102 bacteria were amplified using nested PCR protocols, as previously described (Hu et al. 2014b; Luesken et al.
103 2011b). Nested PCR was that the first PCR products were then used as the DNA templates in the following
104 nested PCR. For 16S rRNA gene amplification, specific forward primer 202F (Ettwig et al. 2009) and general
105 bacterial reverse primer 1545R (Juretschko et al. 1998) were used for the first round, NC10 specific primers

106 qP1F and qP2R (Ettwig et al. 2009) were performed for the second round. For *pmoA* gene amplification,
107 forward primer A189_b and reverse primer cmo682 (Luesken et al. 2011b) were used in the first PCR, and
108 the primer cmo182 and cmo568 were used in the second PCR (Luesken et al. 2011b). The detailed
109 information of nested PCR is shown in Table S1.

110 *Quantitative Real-Time PCR (qPCR)*

111 The quantitative PCR of *M. oxyfera* bacteria 16S rRNA gene were performed on LightCycler480 with
112 Sequence Detection Software v1.4 (Applied Biosystems, USA). The abundance of 16S rRNA gene was
113 determined using the primers qp1R-qp1F (Ettwig et al. 2009) with 10 μL of Power SYBR Green PCR Master
114 Mix (Applied BioSystems), 1 μL of template DNA ($5\text{--}20\text{ ng } \mu\text{L}^{-1}$), 0.4 μL of each primer and 8.2 μL of
115 ddH₂O. Detailed information is exhibited in Table S1. Negative-control reactions in which the DNA
116 template was replaced by nuclease-free water were also performed. The whole process was performed under
117 sterile conditions on ice and away from light. Triplicate qPCR analyses were performed for each sample. The
118 standard curve was constructed from purified plasmid DNA with the concentrations ranging from 1.0×10^1 to
119 1.0×10^7 copies μL^{-1} , and it showed correlation between the DNA template concentration and the crossing
120 point with coefficients of determination ($R^2 > 0.97$). The qPCR amplification efficiency of the standard curve
121 and reactions were both greater than 85%.

122 *Sequencing and phylogenetic analyses*

123 Nucleotide sequences of *M.oxkyfera* bacteria were recovered by 454 high-throughput sequencing (16S rRNA
124 gene) and Illumina MiSeq sequencing (*pmoA* gene), both of which were accomplished by Shanghai
125 Personalbio-pharm Technology Co., Ltd (Shanghai, China). Sequences were clustered into operational
126 taxonomic unites (OTUs) by UCLUST (Edgar et al. 2011). Chao1 richness estimator, ACE estimator, Simpson
127 diversity and Good's coverage were calculated in Mothur analysis (<http://www.mothur.org>). Sequences
128 analyses were operated by BLAST searching to obtain related sequences (>90% identity) from NCBI
129 (<http://www.ncbi.nlm.nih.gov/GenBank/>) and sequence identity was performed in Clustal W version 2.1.
130 Phylogenetic trees were established with MEGA 4.0 software (Tamura et al. 2007) using neighbor-joining
131 method with *p* distance correction and a 1,000-replicate bootstrap value (Hu et al. 2014a).

132 *Nucleotide sequence accession numbers*

133 Sequences obtained from these samples were divided into 16S rRNA and *pmoA* of *M. oxyfera*, and were
134 submitted to GenBank under accession numbers KX153190-KX153201 and KX153202-KX153210,
135 respectively.

136 **Ethical Statement** This article does not contain any studies with human participants or animals performed

137 by any of the authors.

138 **Results**

139 *Physicochemical Characteristics of the Sample Sites*

140 Significant differences in physicochemical characteristics among different environmental samples were
141 observed in the present study. The peak NH_4^+ -N content (815.88 mg N kg^{-1} dry sediment) was detected in WS,
142 which was over 80-folds higher than that in the other three sample sites. And highest NO_2^- -N content (14120
143 mg N kg^{-1} dry sediment) was observed in EC, while NO_2^- -N content in the other three sample site varied from
144 0.37-127.19 mg N kg^{-1} dry sediment. Mainly because of its high NO_2^- content, the highest NO_x^- -N content was
145 also observed in EC, which was beyond 17-folds higher than that of the other three sample sites. In addition,
146 compared with published research conducted in paddy field, where NO_x^- -N content was around 1.4 -3.3 mg N
147 kg^{-1} dry sediment (Shen et al. 2014a; Zhou et al. 2014 ; Ding et al. 2015), higher NO_x^- -N content (27.72 and
148 46.81 mg N kg^{-1} dry sediment) in the agriculture field (PF and CF) of northern China were observed in this
149 study, mainly caused by difference in farming methods.

150 *Abundance of *M.oxyfera* bacteria*

151 FISH analysis was used to investigate the spatial distribution and relative quantification of *M. oxyfera* bacteria
152 compared to total bacteria. As shown in Fig. 1, *M. oxyfera* bacteria (represented by red color) were observed in
153 all four sample sites, and the proportion of *M. oxyfera* bacteria to total bacteria followed the order of
154 EC>PF>CF>WS. Notably, compared with total bacteria, *M. oxyfera* bacteria in the enrichment culture took up
155 over 50%, indicating the predominance of *M. oxyfera* bacteria.

156 To further accurately quantify the abundance of *M. oxyfera* bacteria, qPCR analysis was conducted and
157 significant difference was also observed in different sampling sites. The abundance of *M. oxyfera* bacteria were
158 $7.28 \pm 0.8 \times 10^7$, $1.55 \pm 0.3 \times 10^7$, $1.07 \pm 0.3 \times 10^{10}$, $2.61 \pm 0.1 \times 10^6$ copies per gram of dry sediment in PF, CF, EC and
159 WS, respectively (Fig.2). This order was in consistence with results of FISH analysis.

160

161 **Fig. 1** FISH image of the collected samples. The *M. oxyfera* bacteria was hybridized with probe S⁻-DBACT-1027-a-A-18(Cy3,
162 red) and total bacteria was hybridized with probes EUB I-III (FITC, green). a&e, PF; b&f, CF; c&g, EC, d&h, WS. The scale
163 bar indicates 100 μ m.

164

165 **Fig. 2** The abundance of *M. oxyfera* bacteria in different sample sites.

166 **Potential Rates of n-damo Activity**

167 In order to estimate the activity of *M. oxyfera* bacteria, two groups of experiments were operated using the
168 collected samples, and the results are shown in Fig. 3. In experimental groups amended with CH₄ and NO₂⁻,

169 dramatic decline in CH₄ concentration were observed compared with the blank groups, indicating that CH₄
170 oxidation was propelled by NO₂⁻ reduction under anoxic conditions. The detected anaerobic methane oxidizing
171 rates were 3.90±0.05, 2.58±0.08, 22.31±0.02 and 1.61±0.01 μmol CH₄ g⁻¹ d⁻¹ in PF, CF, EC and WS,
172 respectively. The stoichiometric ratio for methane to nitrite, calculated through the curve fitting method, were
173 3:5.7 for PF, 3:4.6 for CF, 3:6.9 for EC, and 3:3.2 for WS. The value of n-damo enrichment culture was the
174 closest to the theoretical stoichiometric ratio, which was 3:8 (Ettwig et al. 2010).

175

176 **Fig. 3** *The consumption rates of methane and nitrite in the paddy field (a), corn field (b), n-damo enrichment culture (c), WWTP*
177 *(d).*

178 **Sequencing analysis of *M. oxyfera* bacteria 16S rRNA gene**

179 In order to estimate the distribution and composition of *M. oxyfera* bacteria, 454 high-throughput sequencing
180 analysis of 16S rRNA gene was conducted. Raw reads obtained from four libraries ranged from 11017 to
181 14814 and the good coverage values varied from 86.48% to 94.70% (Table S2), indicating that these sequences
182 were enough to analyze the microbial communities. The number of OTUs, Chao1 estimator, ACE estimator,
183 Shannon index and Simpson index based on 97% of the similar level were calculated (Table S2) to estimate
184 the community diversity.

185 The composition of bacteria community in four samples was described at the phylum level (Fig. S1). Some

186 sequences that could not be divided into any known group were classified into others. The first 7 phyla
187 obtained in four sample sites were *NC10*, *Acidobacteria*, *Armatimonadetes*, *Firmicutes*, *Proteobacteria*,
188 *Nitrospirae*, *Verrucomicrobia*. *NC10*, *Acidobacteria* and *Armatimonadetes* were recognized as dominant phyla
189 since they accounting for 93.25% to 99.14% of total bacteria in all samples. For the better understanding of
190 the diversity of *M. oxyfera* bacteria, phylogenetic tree based on selecting all the sequences related to
191 *Candidatus* 'Methylomirabilis oxyfera' (similarities to *M. oxyfera* >90 %) was constructed and is shown in
192 Fig. 4. Sequences of *M. oxyfera* bacteria 16S rRNA gene were grouped into two groups according to Ettiwig et
193 al.(2009) Sequences of group A, which were obtained from PF, CF, EC and WS, showed identity of 94.84-
194 99.31%, 94.20-99.17%, 94.47-99.31%, and 94.16-99.31% to the 16S rRNA gene of *M. oxyfera* bacteria,
195 respectively. Sequences of group B, acquired from the EC showed identity of 89.15% to the 16S rRNA gene of
196 *M. oxyfera* bacteria.

197

198 **Fig. 4** Phylogenetic tree showing the phylogenetic affiliations of *M. oxyfera* bacteria 16S rRNA sequences in different sample
199 sites by neighbor-joining method. Bootstrap values were 1,000 replicates and the scale bar represents 2% of the sequence
200 divergence.

201 **Sequencing analysis of *M. oxyfera* bacteria *pmoA* gene**

202 The Illumina MiSeq sequencing analysis was used to detect the *pmoA* genes of *M. oxyfera* bacteria on a

203 functional level. Raw reads obtained from four libraries ranged from 63,186 to 96,276 and good's coverage
204 varied from 93.91 to 98.13%, indicating that the obtained sequences were able to confirm the bacteria
205 community structure on a functional level. The number of OTUs, Chao1 estimator, ACE estimator, Shannon
206 index and Simpson index based on 97% of the similar level were shown in Table S2.

207 The sequences, which were similar to the *pmoA* gene of *M. oxyfera*, were obtained to construct phylogenetic
208 tree, as shown in Fig. 5. Sequences recovered from PF, CF, EC and WS showed 89.76-91.4%, 90.3-92.7%,
209 89.8-91.4%, 90.3-91.4% of similarity to the *pmoA* gene of *M. oxyfera* bacteria, respectively.

210

211 *Fig. 5 Neighbor-joining phylogenetic tree showing the phylogenetic affiliations of M. oxyfera bacteria pmoA gene sequences in*
212 *different sample sites. Bootstrap values were 1,000 replicates and the scale bar represents 5% of the sequence divergence.*

213

214 Discussion

215 In the present study, PF, CF, EC and WS in northern China, as previously overlooked sites, were selected to
216 investigate the presence and characteristics of n-damo process. Results showed that EC had the highest
217 potential n-damo rate, as well as the highest abundance of *M. oxyfera* bacteria. Correlation analysis showed
218 that the potential n-damo rates and the abundance of *M. oxyfera* bacteria followed the same descending order,
219 i.e., EC>PF>CF>WS, indicating positive correlation between the two indexes. Moreover, the measured

220 potential n-damo rate ($22.31 \pm 0.02 \mu \text{ mol CH}_4 \text{ g}^{-1} \text{ d}^{-1}$) in EC of the present study was higher than that reported
221 in other n-damo enrichment culture ($0.8 \pm 0.1 \mu \text{ mol CH}_4 \text{ h}^{-1} \text{ g}^{-1} \text{ VSS}$) (He et al. 2014). This was attributed to
222 the relative higher abundance of *M. oxyfera* bacteria in the present study. The abundance of *M. oxyfera*
223 bacteria in the present study was over 20 times higher than that reported by He et al. (2014), which verified
224 the positive correlation between the potential n-damo rates and the abundance of *M. oxyfera* bacteria on the
225 other hand.

226 WWTP showed lower abundance of *M. oxyfera* bacteria than the other three sample sites, mainly because
227 of its short biomass retention time (13 days), while biomass retention time of other three sample sites was
228 years or even decades of years (Kampman et al. 2014; Weiland BP. 2006). With the doubling time of 1–2
229 weeks (Ettwig et al. 2009), the growth rate of *M. oxyfera* bacteria is very low, indicating that *M. oxyfera*
230 bacteria might be washed out in WWTP and resulted in lower abundance of *M. oxyfera* bacteria. Another
231 possible reason was that high NH_4^+ content in WWTP, which was unfavorable for the growth of *M. oxyfera*
232 bacteria. Winkler et al. (2015) found that the anammox bacteria had advantage over *M. oxyfera* bacteria for
233 nitrite in the presence of excess ammonium. What is more interesting, although WS was used as initial
234 inoculum for EC in this study, the abundance of *M. oxyfera* bacteria in EC was over 4×10^3 times higher than
235 that in WS. This was mainly attributed to a combination of low NH_4^+ content and high NO_2^- content during
236 the enrichment period in EC. It was reported that the nitrite affinity constant of was $0.6 \text{ g NO}_2^- \cdot \text{Nm}^{-3}$,

237 indicating that high NO_2^- content was more beneficial for the growth of *M. oxyfera* bacteria (Winkler et al.
238 2015).

239 The diversity of *M. oxyfera* bacteria was determined by 16S rRNA gene sequencing analysis. Group A of
240 *M. oxyfera* bacteria, which were the dominant bacteria responsible for conducting the n-damo process (Ettwig
241 et al. 2009; Hu et al. 2009; Luesken et al. 2011a), were obtained in all four sample sites, whereas the group B
242 members were primarily recovered from EC. Sequencing analysis found that diversity of *M. oxyfera* bacteria
243 in PF and CF was higher than that in WS. There is no doubt that PF and CF were believed to be better
244 inoculum to enrich *M. oxyfera* bacteria due to their higher abundance and diversity of *M. oxyfera* bacteria.
245 Notably, with WS used as initial inoculum, increase of 3 OTUs was observed in n-damo EC after cultivation.
246 Besides the optimum enrichment culture in EC, i.e., low NH_4^+ and high NO_2^- contents, which was favorable
247 for the growth of *M. oxyfera* bacteria, the increase in diversity might also be attributed to the longer biomass
248 retention time of EC.

249 The diversity of *M. oxyfera* bacteria *pmoA* gene observed in agriculture fields (PF and CF) were 6 and 7
250 OTUs, respectively, which were higher than most of the previously examined freshwater habitats, including
251 wetland (Hu et al. 2014b; Shen et al. 2015), paddy soil (Shen et al. 2014a) and lake (Deutzmann & Schink
252 2011). And, phylogenetic analysis showed that all the OTUs of *M. oxyfera* bacteria *pmoA* genes in natural
253 environment samples (i.e., PF, CF and WS) of the present study have close genetic relationship with Yellow

254 River basin sediment. Results of 16S rRNA gene sequencing analysis also showed that over half of the OTUs
255 of *M.oxyfera* bacteria 16S rRNA gene obtained in natural environment samples were genetically belongs to the
256 Yellow River basin sediment. This indicated that the diversity of *M. oxyfera* bacteria might be related to
257 geographical regions. Different geographical region has specific environmental conditions, including salinity
258 (Chen et al. 2014), temperature (Hu et al. 2009), pH (He et al. 2015), and etc., all of which would affect the
259 diversity of *M.oxyfera* bacteria. However, further research and more direct evidence are needed to get this
260 conclusion.

261 In conclusion, the present study further expanded our knowledge on distribution and characteristic of *M.*
262 *oxyfera* bacteria in northern China. Comparative analysis showed that long biomass retention time and
263 optimum environment (i.e., low NH_4^+ and high NO_2^- contents) would benefit the growth of *M. oxyfera* bacteria.
264 The diversity of *M. oxyfera* bacteria might also be related to geographical regions. In addition, positive
265 correlation between abundance of *M. oxyfera* bacteria and potential n-damo activity rate were observed.

266 References

- 267 APHA. 2005. Standard methods for the examination of water and wastewater. *American Public Health*
268 *Association (APHA): Washington, DC, USA.*
- 269 Barnes RO, and Goldberg ED. 1976. Methane production and consumption in anoxic marine sediments.
270 *Geology* 4. 10.1130/0091-7613(1976)4<297:mpacia>2.0.co;2

- 271 Bian L, Hinrichs K-U, Xie T, Brassell SC, Iversen N, Fossing H, Jørgensen BB, and Hayes JM. 2001. Algal
272 and archaeal polyisoprenoids in a recent marine sediment: Molecular isotopic evidence for anaerobic
273 oxidation of methane. *Geochemistry, Geophysics, Geosystems* 2:n/a-n/a. 10.1029/2000gc000112
- 274 Cai Z. 2012. Greenhouse gas budget for terrestrial ecosystems in China. *Science China Earth Sciences* 55:173-
275 182. 10.1007/s11430-011-4309-8
- 276 Chen J, Jiang X-W, and Gu J-D. 2014. Existence of Novel Phylotypes of Nitrite-Dependent Anaerobic
277 Methane-Oxidizing Bacteria in Surface and Subsurface Sediments of the South China Sea.
278 *Geomicrobiology Journal* 32:1-10. 10.1080/01490451.2014.917742
- 279 Cui M, Ma A, Qi H, Zhuang X, and Zhuang G. 2015. Anaerobic oxidation of methane: an “active” microbial
280 process. *MicrobiologyOpen* 4:1-11. 10.1002/mbo3.232
- 281 Daims H, Brühl A, Amann R, Schleifer K-H, and Wagner M. 1999. The Domain-specific Probe EUB338 is
282 Insufficient for the Detection of all Bacteria: Development and Evaluation of a more Comprehensive
283 Probe Set. *Systematic and Applied Microbiology* 22:434-444. 10.1016/s0723-2020(99)80053-8
- 284 Deutzmann JS and Schink B. 2011. Anaerobic oxidation of methane in sediments of Lake Constance, an
285 oligotrophic freshwater lake. *Appl Environ Microbiol.* p 4429-4436.
- 286 Ding J, Fu L, Ding ZW, Lu YZ, Cheng SH and Zeng RJ. 2015. "Environmental evaluation of coexistence of
287 denitrifying anaerobic methane-oxidizing archaea and bacteria in a paddy field." *Appl Microbiol*
288 *Biotechnol* 100(1): 439-446.
- 289 Edgar RC, Haas BJ, Clemente JC, Quince C, and Knight R. 2011. UCHIME improves sensitivity and speed of
290 chimera detection. *Bioinformatics* 27:2194-2200.
- 291 Egger M, Rasigraf O, Sapart CJ, Jilbert T, Jetten MSM, Röckmann T, van der Veen C, Bândă N, Kartal B,
292 Ettwig KF, and Slomp CP. 2015. Iron-Mediated Anaerobic Oxidation of Methane in Brackish Coastal

- 293 Sediments. *Environmental Science & Technology* 49:277-283. 10.1021/es503663z
- 294 Emily J. Beal CHH, Victoria J. Orphan. 2009. Manganese- and Iron-Dependent Marine Methane Oxidation.
- 295 Ettwig KF, Butler MK, Le Paslier D, Pelletier E, Mangenot S, Kuypers MM, Schreiber F, Dutilh BE, Zedelius
- 296 J, de Beer D, Gloerich J, Wessels HJ, van Alen T, Luesken F, Wu ML, van de Pas-Schoonen KT, Op
- 297 den Camp HJ, Janssen-Megens EM, Francoijs KJ, Stunnenberg H, Weissenbach J, Jetten MS, and
- 298 Strous M. 2010. Nitrite-driven anaerobic methane oxidation by oxygenic bacteria. *Nature* 464:543-
- 299 548. 10.1038/nature08883
- 300 Ettwig KF, van Alen T, van de Pas-Schoonen KT, Jetten MSM, and Strous M. 2009. Enrichment and
- 301 Molecular Detection of Denitrifying Methanotrophic Bacteria of the NC10 Phylum. *Applied and*
- 302 *Environmental Microbiology* 75:3656-3662. 10.1128/aem.00067-09
- 303 Foley JA, Ramankutty N, Brauman KA, Cassidy ES, Gerber JS, Johnston M, Mueller ND, O'Connell C, Ray
- 304 DK, West PC, Balzer C, Bennett EM, Carpenter SR, Hill J, Monfreda C, Polasky S, Rockstrom J,
- 305 Sheehan J, Siebert S, Tilman D, and Zaks DP. 2011. Solutions for a cultivated planet. *Nature* 478:337-
- 306 342. 10.1038/nature10452
- 307 Griggs DJ, and Noguera M. 2002. Climate change 2001: the scientific basis. Contribution of working group I to
- 308 the third assessment report of the intergovernmental panel on climate change. *Weather* 57:267-269.
- 309 He Z, Cai C, Shen L, Lou L, Zheng P, Xu X, and Hu B. 2014. Effect of inoculum sources on the enrichment of
- 310 nitrite-dependent anaerobic methane-oxidizing bacteria. *Appl Microbiol Biotechnol* 99:939-946.
- 311 10.1007/s00253-014-6033-8
- 312 Hu B, He Z, Geng S, Cai C, Lou L, Zheng P, and Xu X. 2014a. Cultivation of nitrite-dependent anaerobic
- 313 methane-oxidizing bacteria: impact of reactor configuration. *Appl Microbiol Biotechnol* 98:7983-7991.
- 314 10.1007/s00253-014-5835-z

- 315 Hu BL, Shen LD, Lian X, Zhu Q, Liu S, Huang Q, He ZF, Geng S, Cheng DQ, Lou LP, Xu XY, Zheng P, and
316 He YF. 2014b. Evidence for nitrite-dependent anaerobic methane oxidation as a previously
317 overlooked microbial methane sink in wetlands. *Proc Natl Acad Sci U S A* 111:4495-4500.
318 10.1073/pnas.1318393111
- 319 Hu S, Zeng RJ, Burow LC, Lant P, Keller J, and Yuan Z. 2009. Enrichment of denitrifying anaerobic methane
320 oxidizing microorganisms. *Environmental Microbiology Reports* 1:377-384.
- 321 Hu S, Zeng RJ, Keller J, Lant PA, and Yuan Z. 2011. Effect of nitrate and nitrite on the selection of
322 microorganisms in the denitrifying anaerobic methane oxidation process. *Environ Microbiol Rep*
323 3:315-319. 10.1111/j.1758-2229.2010.00227.x
- 324 Intergovernmental Panel on Climate Change (IPCC), *Third Assessment Report. Working Group I*, Cambridge
325 Univ. Press, New York, 2001.
- 326 Juretschko S, Timmermann G, Schmid M, Schleifer K-H, Pommerening-Röser A, Koops H-P, and Wagner M.
327 1998. Combined molecular and conventional analyses of nitrifying bacterium diversity in activated
328 sludge: Nitrosococcus mobilis and Nitrospira-like bacteria as dominant populations. *Applied and*
329 *environmental microbiology* 64:3042-3051.
- 330 Kampman C, Temmink H, Hendrickx TLG, Zeeman G, and Buisman CJN. 2014. Enrichment of denitrifying
331 methanotrophic bacteria from municipal wastewater sludge in a membrane bioreactor at 20°C. *Journal*
332 *of Hazardous Materials* 274:428-435. 10.1016/j.jhazmat.2014.04.031
- 333 Knittel K, and Boetius A. 2009. Anaerobic Oxidation of Methane: Progress with an Unknown Process.
334 *Annual Review of Microbiology*, 311-334.
- 335 Liu Y, Cheng X, Lun X, and Sun D. 2014a. CH₄ emission and conversion from A2O and SBR processes in
336 full-scale wastewater treatment plants. *Journal of Environmental Sciences* 26:224-230.

- 337 [http://dx.doi.org/10.1016/S1001-0742\(13\)60401-5](http://dx.doi.org/10.1016/S1001-0742(13)60401-5)
- 338 Liu Y, Zhang J, Zhao L, Li Y, Yang Y, and Xie S. 2014b. Aerobic and nitrite-dependent methane-oxidizing
339 microorganisms in sediments of freshwater lakes on the Yunnan Plateau. *Appl Microbiol Biotechnol*
340 99:2371-2381. 10.1007/s00253-014-6141-5
- 341 Luesken FA, van Alen TA, van der Biezen E, Frijters C, Toonen G, Kampman C, Hendrickx TLG, Zeeman G,
342 Temmink H, Strous M, Op den Camp HJM, and Jetten MSM. 2011a. Diversity and enrichment of
343 nitrite-dependent anaerobic methane oxidizing bacteria from wastewater sludge. *Appl Microbiol*
344 *Biotechnol* 92:845-854. 10.1007/s00253-011-3361-9
- 345 Luesken FA, Zhu B, van Alen TA, Butler MK, Diaz MR, Song B, Op den Camp HJM, Jetten MSM, and
346 Ettwig KF. 2011b. pmoA Primers for Detection of Anaerobic Methanotrophs. *Applied and*
347 *Environmental Microbiology* 77:3877-3880. 10.1128/aem.02960-10
- 348 Montzka SA, Dlugokencky EJ, and Butler JH. 2011. Non-CO2 greenhouse gases and climate change. *Nature*
349 476:43-50. 10.1038/nature10322
- 350 Raghoebarsing AA, Pol A, van de Pas-Schoonen KT, Smolders AJ, Ettwig KF, Rijpstra WI, Schouten S,
351 Damste JS, Op den Camp HJ, Jetten MS, and Strous M. 2006. A microbial consortium couples
352 anaerobic methane oxidation to denitrification. *Nature* 440:918-921. 10.1038/nature04617
- 353 Ryan J, Estefan G, and Rashid A. 2007. *Soil and plant analysis laboratory manual*. ICARDA.
- 354 Segarra KEA, Comerford C, Slaughter J, and Joye SB. 2013. Impact of electron acceptor availability on the
355 anaerobic oxidation of methane in coastal freshwater and brackish wetland sediments. *Geochimica et*
356 *Cosmochimica Acta* 115:15-30. 10.1016/j.gca.2013.03.029
- 357 Shen L-d, Liu S, He Z-f, Lian X, Huang Q, He Y-f, Lou L-p, Xu X-y, Zheng P, and Hu B-l. 2015. Depth-
358 specific distribution and importance of nitrite-dependent anaerobic ammonium and methane-oxidising

- 359 bacteria in an urban wetland. *Soil Biology and Biochemistry* 83:43-51.
360 <http://dx.doi.org/10.1016/j.soilbio.2015.01.010>
- 361 Shen L-d, Liu S, Huang Q, Lian X, He Z-f, Geng S, Jin R-c, He Y-f, Lou L-p, and Xu X-y. 2014a. Evidence
362 for the cooccurrence of nitrite-dependent anaerobic ammonium and methane oxidation processes in a
363 flooded paddy field. *Applied and environmental microbiology* 80:7611-7619.
- 364 Shen L-d, Qun Z, Shuai L, Ping D, Jiang-ning Z, Dong-qing C, Xiang-yang X, Ping Z, and Bao-lan H. 2014b.
365 Molecular evidence for nitrite-dependent anaerobic methane-oxidising bacteria in the Jiaojiang
366 Estuary of the East Sea (China). *Appl Microbiol Biotechnol* 98:5029-5038. 10.1007/s00253-014-5556-
367 3
- 368 Smemo KA, and Yavitt JB. 2007. Evidence for Anaerobic CH₄ Oxidation in Freshwater Peatlands.
369 *Geomicrobiology Journal* 24:583-597. 10.1080/01490450701672083
- 370 Syakila A, and Kroeze C. 2011. The global nitrous oxide budget revisited. *Greenhouse Gas Measurement and*
371 *Management* 1:17-26. 10.3763/ghgmm.2010.0007
- 372 Tamura K, Dudley J, Nei M, and Kumar S. 2007. MEGA4: molecular evolutionary genetics analysis (MEGA)
373 software version 4.0. *Molecular biology and evolution* 24:1596-1599.
- 374 Wang J, Zhang J, Wang J, Qi P, Ren Y, and Hu Z. 2011a. Nitrous oxide emissions from a typical northern
375 Chinese municipal wastewater treatment plant. *Desalination and Water Treatment* 32:145-152.
376 10.5004/dwt.2011.2691
- 377 Wang J, Zhang J, Xie H, Qi P, Ren Y, and Hu Z. 2011b. Methane emissions from a full-scale A/A/O
378 wastewater treatment plant. *Bioresource Technology* 102:5479-5485. 10.1016/j.biortech.2010.10.090
- 379 Wang Y, Zhu G, Harhangi HR, Zhu B, Jetten MSM, Yin C, and Op den Camp HJM. 2012. Co-occurrence and
380 distribution of nitrite-dependent anaerobic ammonium and methane-oxidizing bacteria in a paddy soil.

- 381 *FEMS Microbiology Letters* 336:79-88. 10.1111/j.1574-6968.2012.02654.x
- 382 Weiland BP. 2006. Biomass Digestion in Agriculture: A Successful Pathway for the Energy Production and
383 Waste Treatment in Germany. *Engineering in Life Sciences* 6:302-309. 10.1002/elsc.200620128
- 384 Winkler MKH, Ettwig KF, Vannecke TPW, Stultiens K, Bogdan A, Kartal B, and Volcke EIP. 2015.
385 Modelling simultaneous anaerobic methane and ammonium removal in a granular sludge reactor.
386 *Water Research* 73:323-331. 10.1016/j.watres.2015.01.039
- 387 Zhou LL, Wang Y, Long XE, Guo JH, Zhu GB. 2014. "High abundance and diversity of nitrite-dependent
388 anaerobic methane-oxidizing bacteria in a paddy field profile." *FEMS Microbiology Letters* 360(1):
389 33-41.
- 390
- 391

Table 1 (on next page)

Environmental characteristics

Environmental characteristics of the sample sites.

1 **Distribution and characteristic of nitrite-dependent anaerobic methane oxidation bacteria in wastewater**
2 **treatment plants and agriculture fields of northern China**

3 **Ru Ma . Zhen Hu***

4 Shandong Provincial Key Laboratory of Water Pollution Control and Resource Reuse, School of
5 Environmental Science and Engineering, Shandong University, No. 27 Shanda South Road, Jinan 250100,
6 Shandong, People's Republic of China. E-mail: huzhen885@sdu.edu.cn

7 **Table 1.** Environmental characteristics of the sample sites.

Sample sites	Geographic coordinates	Temperature (°C)	pH	Ammonium (mg N/kg dry sed)	Nitrite (mg N/kg dry sed)	Nitrate (mg N/kg dry sed)	Salinity (‰)
PF	N36° 41', E116° 54'	17	7.3	10.34	0.75	26.97	1.8
CF	N37° 44', E115° 40'	15	7.0	2.627	0.37	46.44	1.1
EC	N36° 40', E117° 03'	32	7.0	0.125	14117.65	941.18	1.2
WS	N36° 42', E117° 02'	22	7.6	815.88	127.19	735.29	2.1

8

9

10

Figure 1(on next page)

FISH image of the collected samples.

Fig. 1- FISH image of the collected samples. The *M. oxyfera* bacteria was hybridized with probe S^{*}-DBACT-1027-a-A-18(Cy3, red) and total bacteria was hybridized with probes EUB I-III (FITC, green). a&e, PF; b&f, CF; c&g, EC, d&h, WS. The scale bar indicates 100 µm.

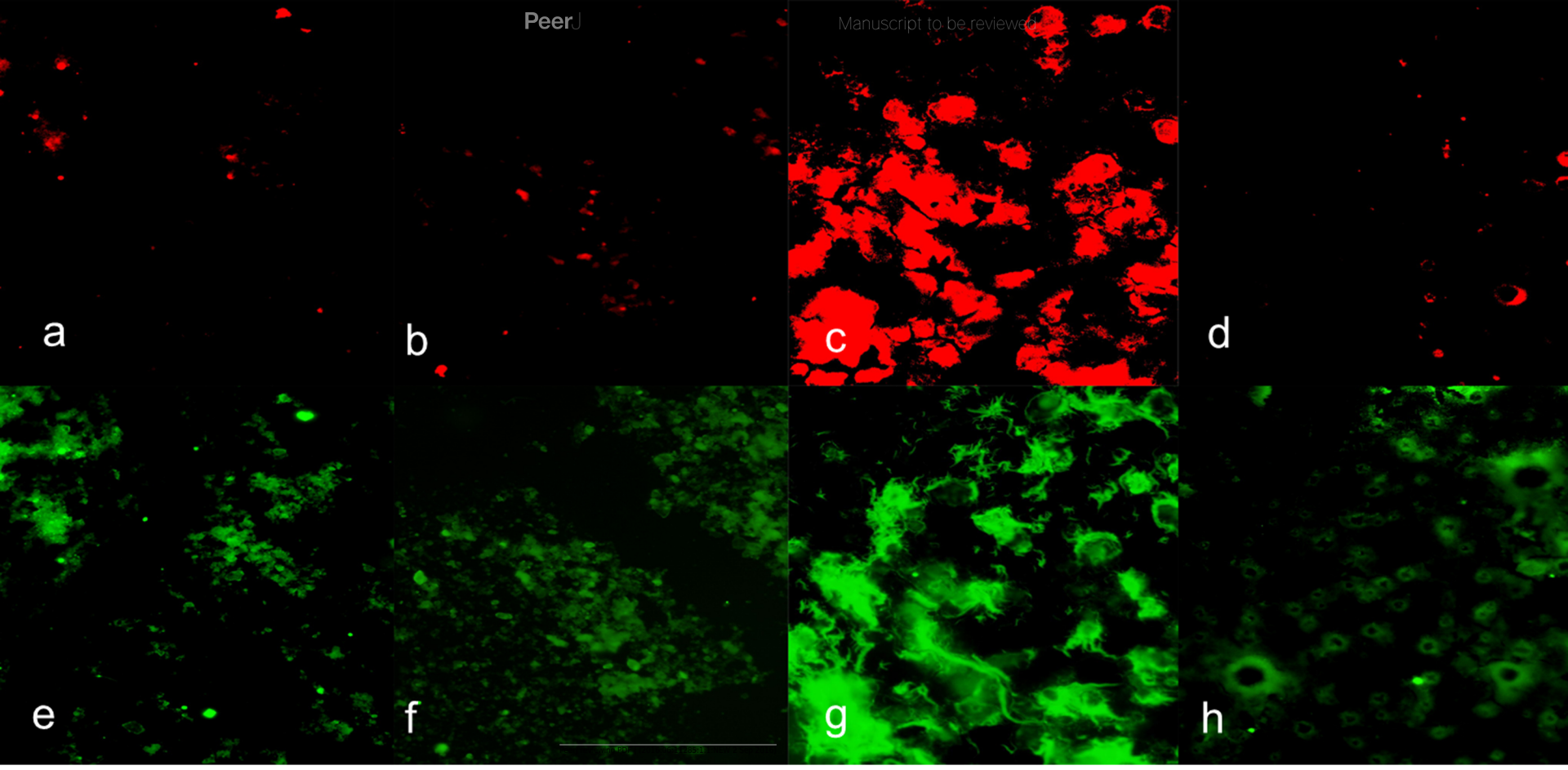


Figure 2 (on next page)

Q-PCR Image of *M. oxyfera* bacteria

Fig. 2- The abundance of *M. oxyfera* bacteria 16S rRNA gene copy numbers of collected samples.

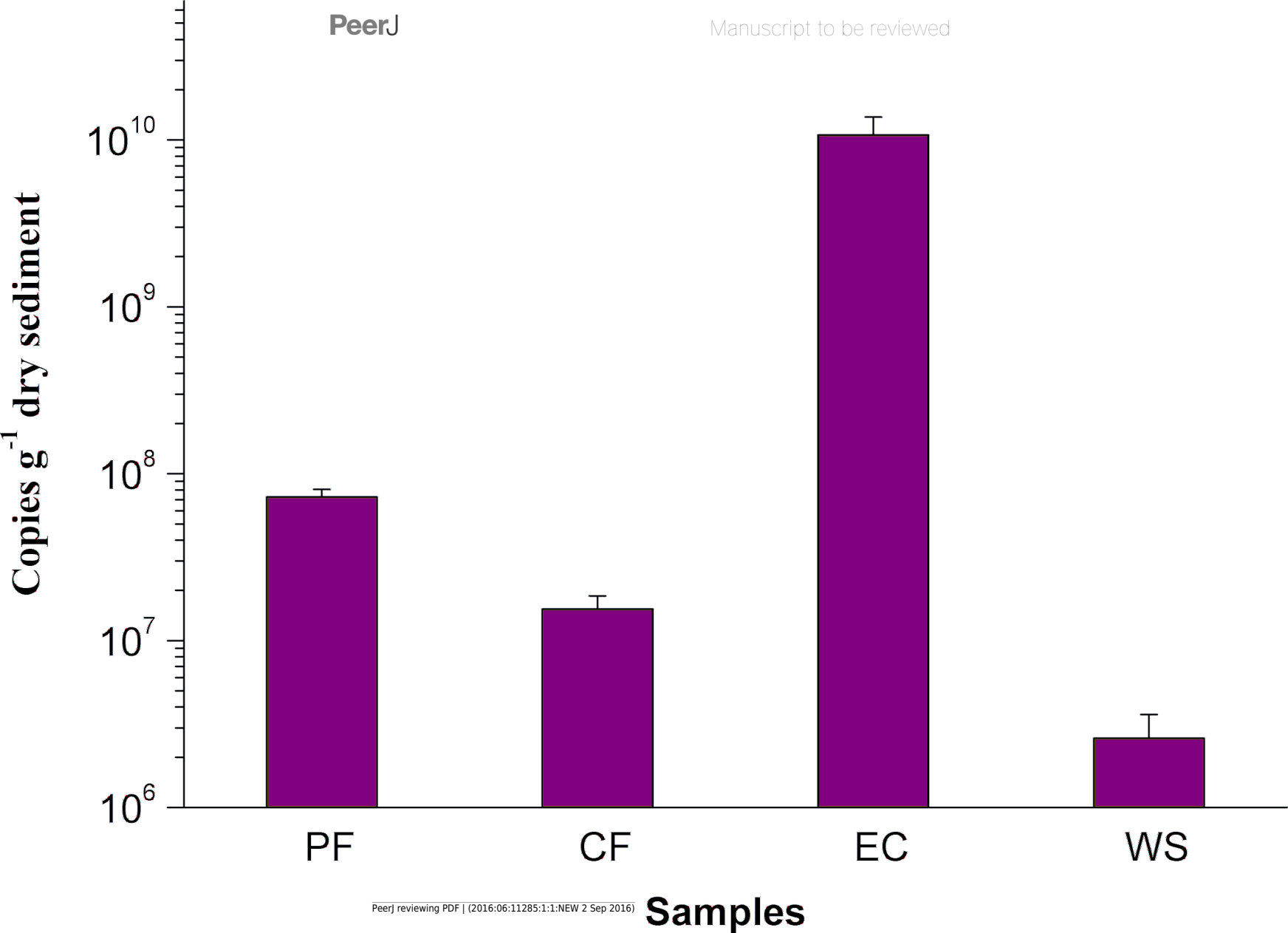


Figure 3 (on next page)

Image of batch test

Fig. 3 The consumption rates of methane and nitrite in the paddy field (a), corn field (b), n-damo enrichment culture (c), WWTP (d).

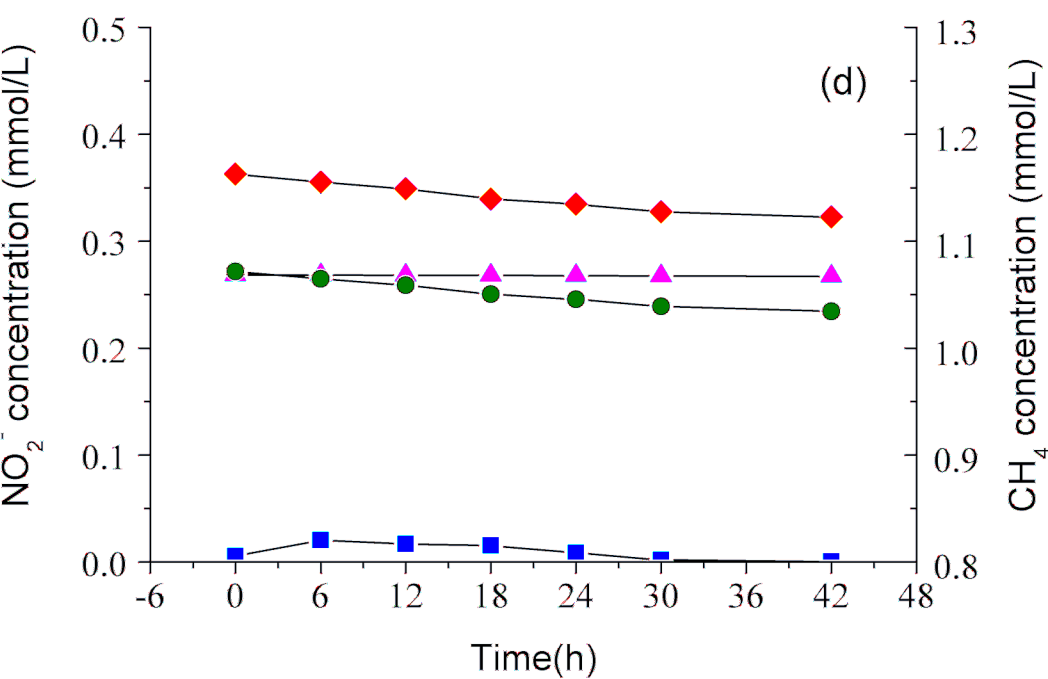
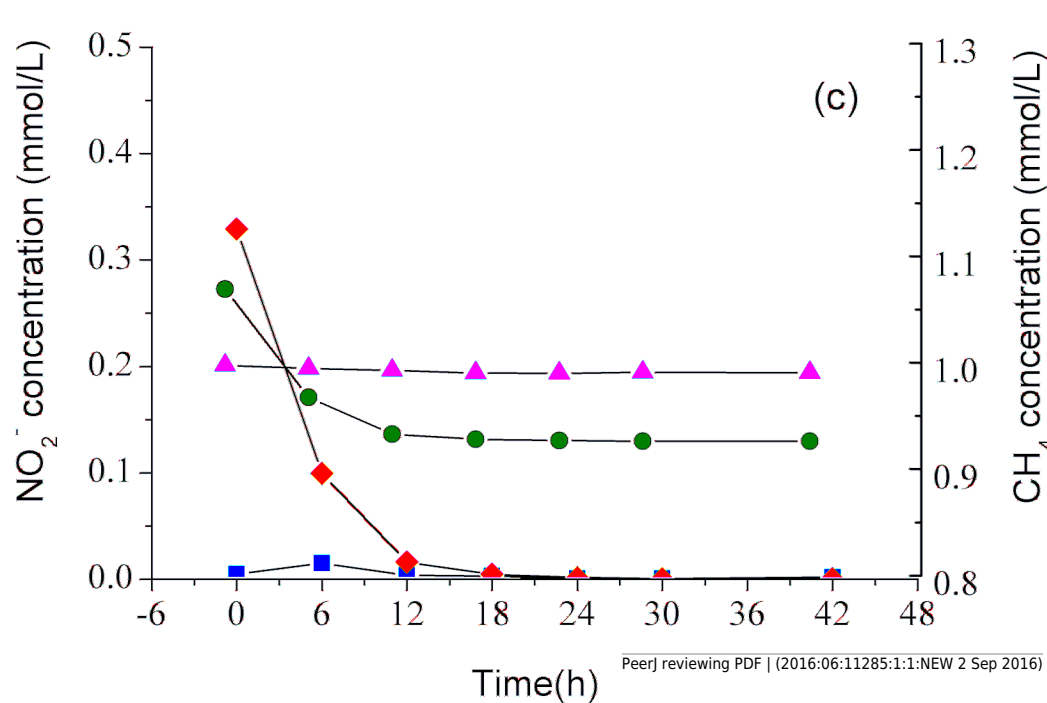
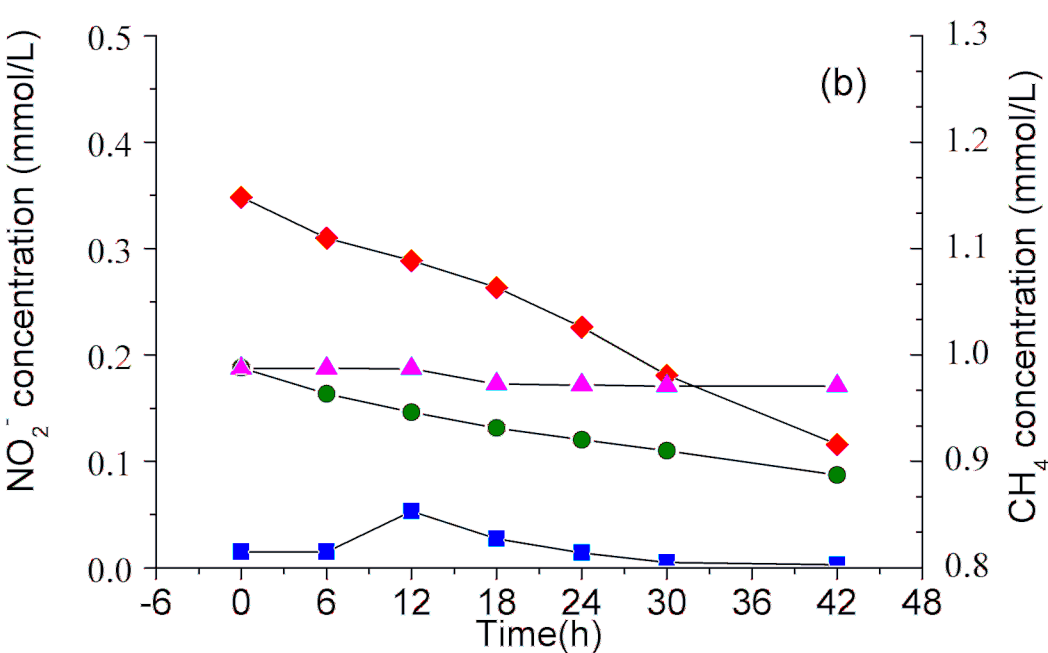
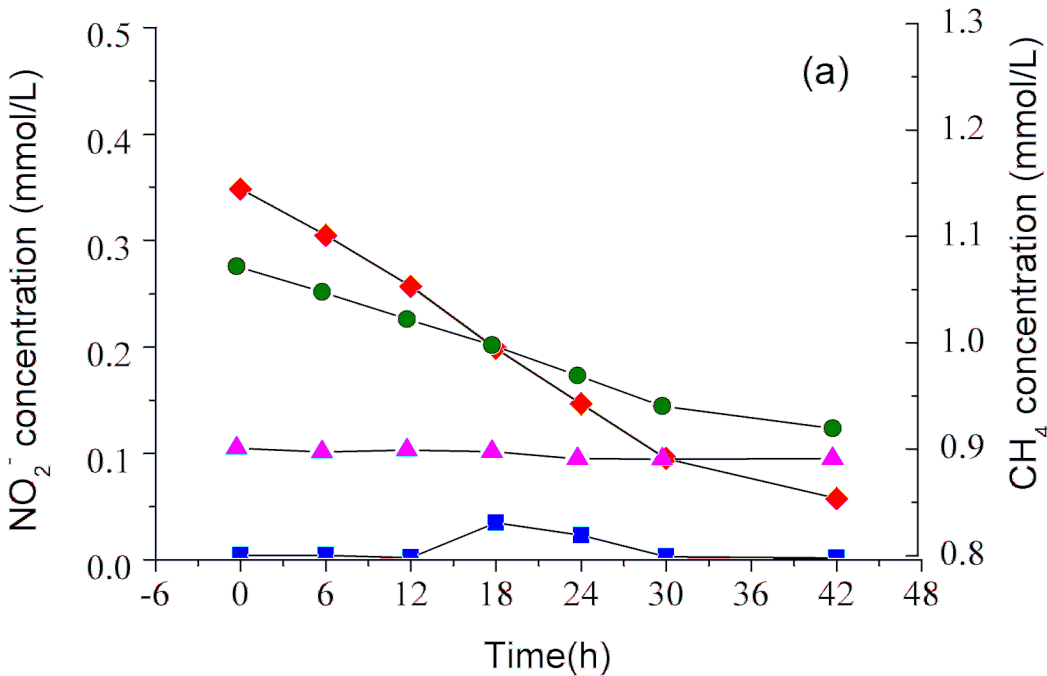


Figure 4(on next page)

Phylogenetic tree of *M. oxyfera* bacteria 16S rRNA sequences

Fig. 4 - Phylogenetic tree showing the phylogenetic affiliations of *M. oxyfera* bacteria 16S rRNA sequences in four samples by neighbor-joining method. Bootstrap values were 1,000 replicates and the scale bar represents 2% of the sequence divergence.

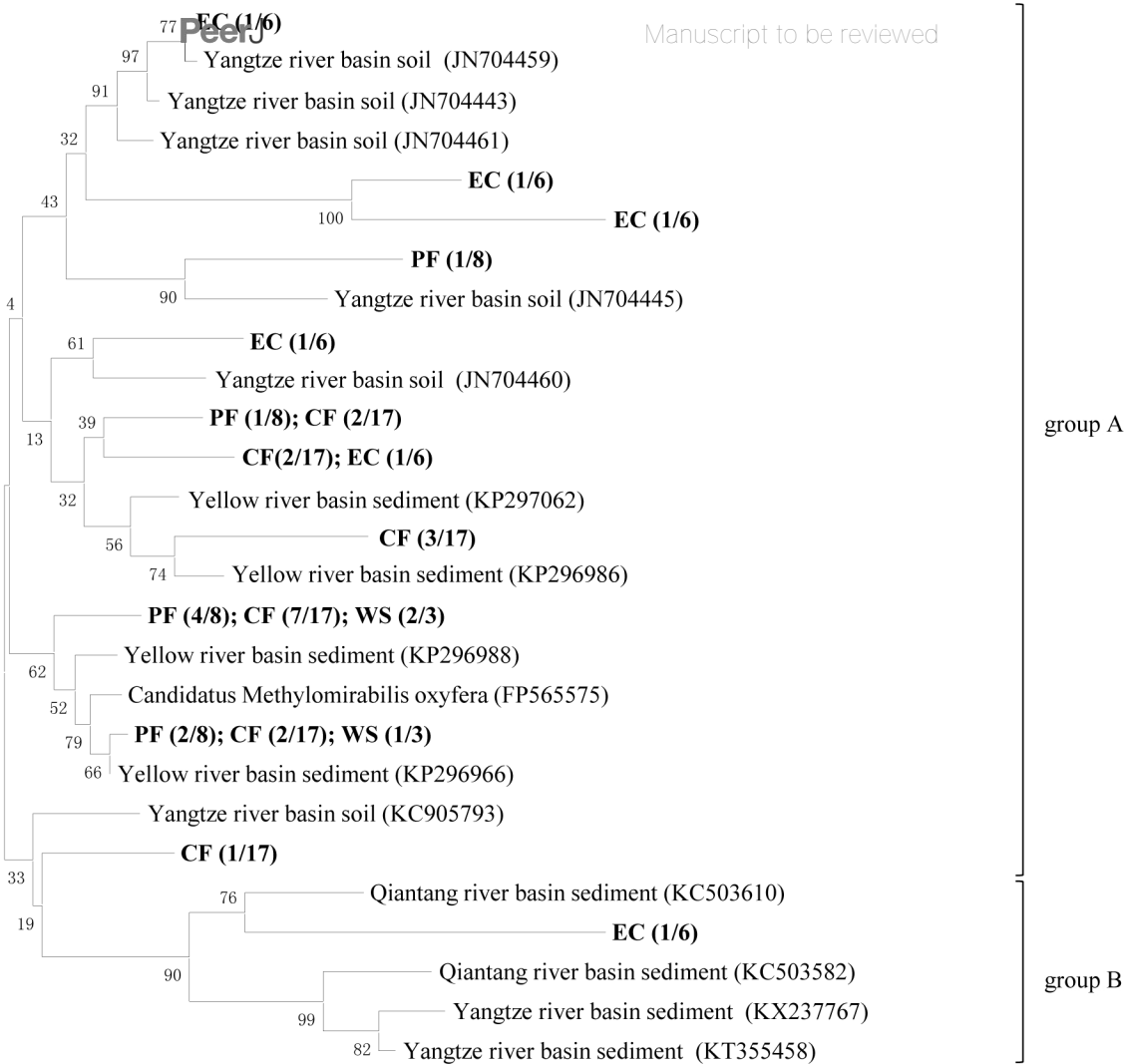


Figure 5 (on next page)

Phylogenetic tree of *M. oxyfera* bacteria *pmoA* gene

Fig. 5 - Neighbor-joining phylogenetic tree showing the phylogenetic affiliations of *M. oxyfera* bacteria *pmoA* gene sequences in four samples. Bootstrap values were 1,000 replicates and the scale bar represents 5% of the sequence divergence.

